

Photonic crystal laser with mode selective mirrors

S. A. Moore, L. O'Faolain, T. P. White and T. F. Krauss

*Department of Physics and Astronomy, University of St Andrews, St Andrews,
Fife, KY16 9SS, UK*

sam15@st-andrews.ac.uk

Abstract: The mini-stopband (MSB) of a W3 line-defect photonic crystal waveguide is used as a mirror for a GaAs based quantum-dot laser. Single mode, continuous-wave lasing is demonstrated for broad area lasers up to a current of 125 mA (2.7 x laser threshold), which demonstrates the high degree of mode selectivity of the MSB mirror. FDTD calculations indicate that optimisation of the mirror interface could lead to a further fourfold increase in reflectivity resulting in significantly reduced thresholds.

© 2008 Optical Society of America

OCIS codes: (140.5960) Semiconductor lasers; (230.7370) Waveguides; (250.5300) Photonic integrated circuits

References and links

1. J. O'Brien, O. Painter, R. Lee, C. C. Cheng, A. Yariv and A. Scherer, "Lasers incorporating 2D photonic bandgap mirrors," *Electron. Lett.* **32**, 2243–2244 (1996).
2. T. F. Krauss, O. Painter, A. Scherer, J. S. Roberts and R. M. De La Rue, "Photonic microstructures as laser mirrors," *Opt. Eng.* **37**, 1143–1148 (1998).
3. A. Talneau, L. LeGratiet, J. L. Gentner, A. Berrier, M. Mulot, S. Anand and S. Olivier, "High external efficiency in a monomode full-photonic-crystal laser under continuous wave electrical injection," *Appl. Phys. Lett.* **85**, 1913–1915 (2004).
4. X. Checoury, P. Crozat, J.-M. Lourtioz, C. Cuisin, E. Derouin, F. Poigt, L. Legouezigou, P. Pommereau, G.-H. Dunn, O. Gauthier-Lafaye, S. Bonnefont, D. Mulin, F. Lozes-Dupuy and A. Talneau, "Single-mode in-gap emission of medium-width photonic crystal waveguides on InP substrate," *Opt. Express* **13**, 6947–6955 (2005).
5. S. A. Moore, L. O'Faolain, M. A. Cataluna, M. B. Flynn, M. V. Kotlyar and T. F. Krauss, "Reduced surface sidewall recombination and diffusion in quantum-dot lasers," *Photon. Technol. Lett.* **8**, 1861–1863 (2006).
6. C. J. M. Smith, H. Benisty, S. Olivier, M. Rattier, C. Weisbuch, T. F. Krauss, R. M. De la Rue, R. Houdre and U. Oesterle, "Low-loss channel waveguides with two-dimensional photonic crystal boundaries," *Appl. Phys. Lett.* **77**, 2813–2815 (2000).
7. S. G. Johnson and J. D. Joannopoulos, "Block-iterative frequency-domain methods for Maxwell's equations in a planewave basis," *Opt. Express* **18**, 173–195 (2001).
8. S. Olivier, M. Rattier, H. Benisty, C. Weisbuch, C. J. M. Smith, R. M. De La Rue, T. F. Krauss, U. Oesterle and R. Houdre, "Mini-stopbands of a one-dimensional system: The channel waveguide in a two-dimensional photonic crystal," *Phys. Rev. B* **63**, 113311 (2001).
9. <http://www.nanophotonics.eu>.
10. S. Olivier, H. Benisty, C. Weisbuch, C. J. M. Smith, T. F. Krauss and R. Houdre, "Coupled-mode theory and propagation losses in photonic crystal waveguides," *Opt. Express* **11**, 1490–1496 (2003).

1. Introduction

Photonic crystals exhibit a photonic band-gap (PBG) that can be used as a high reflectivity laser mirror. This capability was first demonstrated ten years ago using both 2D [1] and 1D [2] deeply etched microstructures. These PBG mirrors are broadband and reflect any mode with a frequency that lies within the band-gap. More recently, lasers with mode filtering were demonstrated by using a photonic crystal waveguide to provide an additional periodicity or mode

folding within the band-gap [3, 4]. As a result, devices exhibited single transverse mode behaviour, but only under pulsed excitation.

In this letter, we take the mode-selective idea further and demonstrate the use of the MSB concept as a stand-alone mirror. In addition, we combine the photonic crystal waveguide with a broad area gain section. As a result, we achieve low threshold currents and very stable single mode operation up to 2.7x threshold, which highlights the potential of the mode-selective mirror to act as both a filter and an effective feedback element for broad area, high power lasers. We used GaAs/InGaAs quantum-dot material that was recently shown to exhibit surface recombination velocity values similar to those of InP [5], thus allowing the fabrication of deeply etched narrow mesa lasers and photonic crystal structures that have little impact on the internal quantum efficiency of the device.

2. Design and fabrication

We used a photonic crystal waveguide created by removing 3 lines of holes from a perfect lattice in the ΓK direction, typically referred to as a W3-type waveguide [6], which exhibits a mini-stopband (MSB) for the fundamental mode. The band-structure of a typical W3-type waveguide is shown in Fig. 1(a), which was calculated with the open source mpb software [7]. A dielectric refractive index of 3.2 and a hole radius of $0.3a$, where a is the period, was used for the 2D calculation. Figure 1(a) shows that several modes are supported within the band-gap that spans from $a/\lambda=0.22$ to 0.29 . Modes of the same parity are seen to interact and therefore anticross [8], e.g. the fundamental and the fourth order mode at $k=0.15$, as highlighted in Fig. 1(b). We designed the spectral region of this MSB to lie in the gain spectrum of the laser material. Since the MSB is the result of the anticrossing between the fundamental and fourth order mode, these modes will be reflected by the W3. The first and second order modes that are most likely to compete with the fundamental for lasing are not reflected and are therefore unlikely to lase.

A layout of the laser and W3 mirror, which are connected by a tapered access waveguide, is shown in Fig. 2(a). The waveguides in the fabricated devices continue beyond the photonic crystal section, and are later used to illustrate the mirror operation of the MSB (Fig. 3(b), 3(c) and 4).

The quantum-dot material and fabrication procedure used in the study are the same as in [5]. The devices were fabricated through the ePIXnet Nanostructuring Platform for Photonic Integration [9]. The etch mask and deeply etched photonic crystal holes are shown in Fig. 2(b) and (c) respectively.

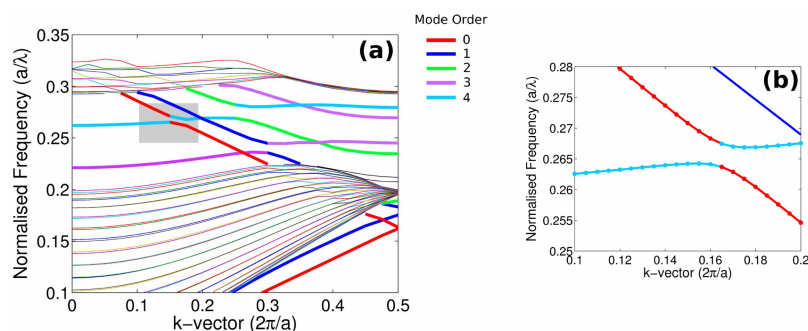


Fig. 1. (a) Band structure of a photonic crystal W3 defect waveguide. (b) Local picture of the MSB arising from the anti-crossing of the fundamental and 4th order modes.

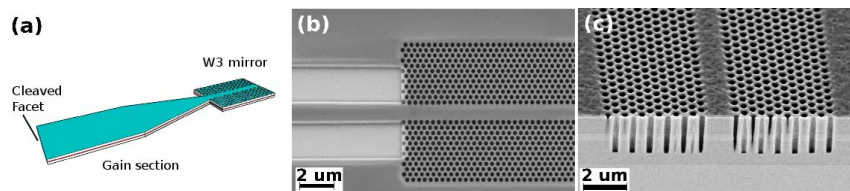


Fig. 2. Overview of structure. (a) Schematic of device (not to scale). The gain section is 1.8 mm long with a 200 μm taper to the W3 mirror (100 periods long). The W3 mirror and 50 μm of the taper are unpumped. The other mirror is a cleaved facet. (b) Patterned electron-beam resist and (c) Deep etching of holes, the waveguiding layer, containing the quantum-dots, can be seen as the lighter horizontal stripe bisecting the holes.

3. Results

As shown in Fig. 1(a), the MSB lies at a normalised frequency of $a/\lambda \sim 0.27$, which corresponds to a period of 345 nm for the peak gain wavelength of the quantum-dot material of 1280 nm. Initially, a passive device with a slightly longer period was fabricated to confirm the exact position of the MSB and its attenuation. The transmission spectrum of a 360 nm period, passive W3-defect waveguide, probed with a Koheras SuperKTM Compact white light source, clearly showed a MSB with a centre wavelength of 1325 nm and a 20dB attenuation. This corresponds to a normalised frequency of $360/1325 \sim 0.272$ in agreement with Fig. 1.

Laser devices with a 5 μm wide gain section were fabricated and mounted p-side up on copper blocks. The devices were probed with a DC current supply and the output analysed with an optical spectrum analyser (OSA) and a power meter. Figure 3(a) shows the P-I curves of 3 devices with W3 mirror periods of 335, 350 and 355 nm. The best curve (355 nm period) shows good laser action with a threshold current of 15.9 mA and a slope efficiency of 0.08 mW/mA from the cleaved facet. The thresholds for both the 350 nm and 355 nm period devices are similar to those of two-facet 5 μm wide mesa devices fabricated with the same material [5]. The 335 nm device has a very poor efficiency of 0.008 mW/mA and over twice the threshold of the other devices. In fact, it is debatable if lasing is occurring at all in the latter.

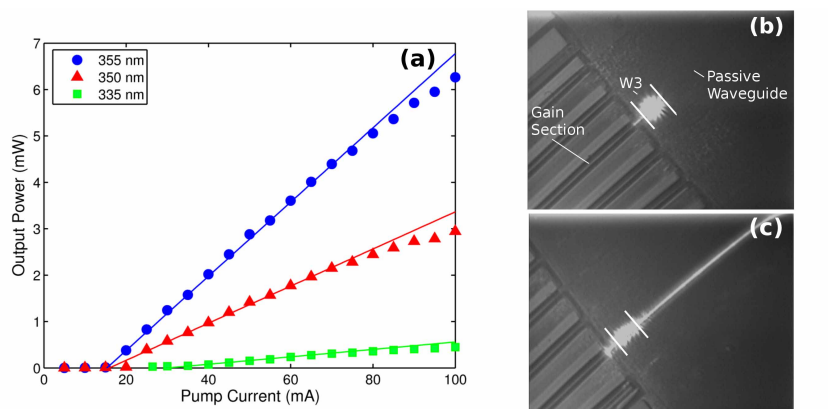


Fig. 3. (a) P-I curve of laser devices with a 335, 350 and 355 nm period W3 mirrors, (b) Top-down camera image of 350 nm device above threshold and (c) Top-down camera image of 335 nm device.

Figure 3(b) shows the top-view IR camera image at the W3 mirror end of the 350 nm period

device. The high reflection of the W3 mirror is clearly visible as the bright spot. No light is seen in the passive waveguide. The 355 nm device had a similar appearance. Figure 3(c) shows the IR camera image for the 335 nm period device. Large amounts of light can be seen entering the passive waveguide which indicates operation away from the MSB of the W3 waveguide.

The OSA showed lasing peaks at 1260 nm and 1280 nm for the 350 nm and 355 nm devices, respectively. It should be noted that the 355 nm device operates at the material peak gain wavelength (1280 nm). This may account for the device having a better slope efficiency than the 350 nm period device as seen in Fig. 3(a). The 355 nm period device lased at the peak gain wavelength (1280 nm) indicating that feedback was provided by mode-mismatch at the W3 interface rather than the MSB at ~ 1200 nm (far from the gain peak). This accounts for the poor laser performance seen in Fig. 3(a) and the light seen in the passive waveguide in Fig. 3(c).

The low thresholds, good slope efficiencies and camera images suggested that the 350 nm and 355 nm period devices were lasing via reflections from the MSB. To confirm this, the back-end of the device was cleaved and the output through the passive waveguide (through the W3 mirror) observed on the OSA. Figure 4 shows these output spectra for the 350 nm and 355 nm devices. The MSB is clearly visible as a broad ~ 20 nm wide dip with the lasing peak evident inside the MSB.

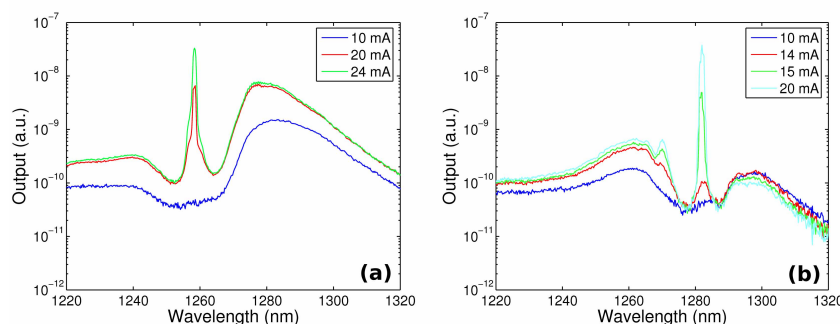


Fig. 4. Spectral output of W3 laser devices transmitted through W3 mirror for (a) 350 nm and (b) 355 nm device.

The major advantage of this type of mirror is its mode selectivity, i.e. it addresses one of the major disadvantages of broad mesa lasers, namely their tendency for multi-mode operation. The MSB only reflects the fundamental and fourth order modes and so even mesa lasers with a broad gain-section should operate as single mode devices (the fourth order mode is unlikely to lase even in a standard broad area laser with two cleaved facets). To highlight this, devices with a $20 \mu\text{m}$ wide gain section were fabricated and characterised. The far field mode-profiles of the collimated beams were measured using a beam profiler. The profile of a device reflecting from a W3 MSB is shown in Fig. 5. Also shown are the profiles for two as-cleaved facet devices. One device has a constant width of $20 \mu\text{m}$ and the other has a taper similar to the one used for the W3. The profiles show that the taper provides some mode filtering compared with the plain $20 \mu\text{m}$ device, but the extra lobes persist. The W3 mirror device is the only one that has a single lobe throughout the operating range, highlighting the mode selective feedback obtained from the MSB.

4. Design improvement

The data above clearly indicates the mode selectivity of the MSB mirror, but considering the strong transmission dip seen in the passive measurement, one would also expect higher reflect-

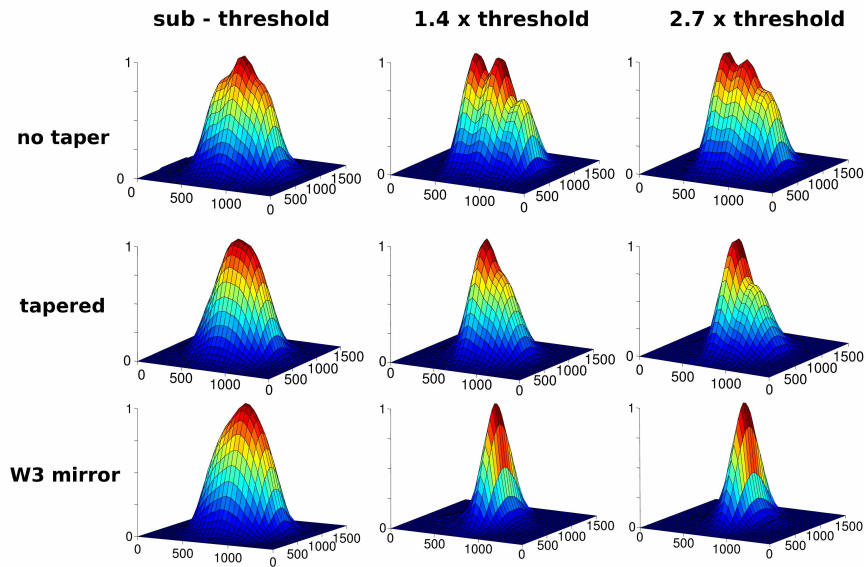


Fig. 5. Mode profiles of devices at sub-threshold, $1.4 \times$ threshold and $2.7 \times$ threshold for un-tapered $20 \mu\text{m}$, tapered $20 \mu\text{m}$ and W3 mirrored $20 \mu\text{m}$ wide devices. The horizontal axes are displacement across the beam (μm). The threshold current density was very similar for all devices.

tivity than from a cleaved facet and correspondingly lower thresholds. These are not observed. The reflection from a MSB is more complex than being directly related to transmission and involves modal conversion between the fundamental and fourth order modes of the W3 [10].

To investigate this issue, we performed 2D finite difference time domain (FDTD) simulations to study the back-reflection from the W3 waveguide into the tapered access waveguide. The holes are etched to a depth $1.5 \mu\text{m}$ below the waveguide core and were calculated to overlap with 99.9996% of the guided mode, justifying the "infinitely deep hole" assumption inherent in a 2D calculation. A W3 waveguide length of 20 periods was used to increase simulation speed. Initially, the simulation was run for the parameters of the devices fabricated above with the fundamental mode of the access waveguide incident on the W3 (Fig. 6(a) inset). We found that $\sim 15\%$ of the incident light was coupled back into the fundamental mode of the access waveguide and $\sim 15\%$ was coupled into the fourth order mode of the access waveguide with negligible light coupling to other modes. The field profile (Fig. 6(c)) shows significant scattering away from the waveguide, indicating inefficient coupling at the W3 interface.

In order to address this issue and improve the interface coupling, the width of the access guide was varied. The simulated results in Fig. 6(a) show reflection into the fundamental mode of the access waveguide as a function of access waveguide width. The x-axis units are normalised to the width of a W3 (width $w = 2\sqrt{3}a$). For a normalised access guide width of $w=1$ (experimental value (highlighted)), the access guide terminates in the centre of the boundary holes of the W3 waveguide. As the access waveguide is narrowed, the reflection first falls to a minimum at $w \sim 0.9 \times W3$. At this value, the edges of the access waveguide are in line with the edge of the first row of holes of the W3. This suggests that scattering is the main mechanism preventing coupling of reflected light back into the access waveguide. However, by narrowing the access waveguide further, the reflectivity into the fundamental mode of the access waveguide increases again and peaks at a width of $w \sim 0.7 \times W3$. The field profile at this access guide

width (Fig. 6(b)) shows efficient coupling and little scattering. We can therefore increase the reflectivity into the fundamental mode by up to a factor of 4 over the present value, which should lead to a significant decrease in threshold current.

It should be noted that this optimum coupling width for the W3 waveguide is different to the optimum access waveguide width for a W1 waveguide. For a W1 waveguide, the access waveguide is typically the same width as the W1, i.e. it terminates in the centre of the first row of holes. Our simulation shows that this termination, surprisingly, is not the optimal coupling width for maximum back-reflection from a W3 waveguide into the fundamental mode.

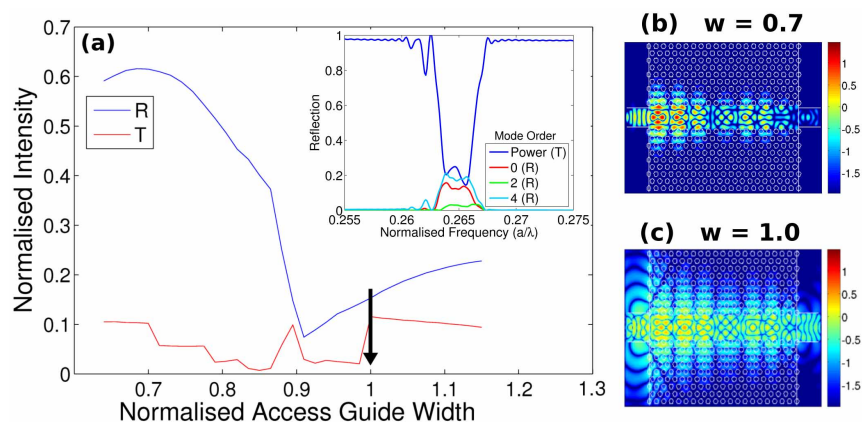


Fig. 6. (a) Simulated Reflection and Transmission through variation of access guide width. The region corresponding to the experimental results is highlighted with an arrow. Inset: Spectral reflection for normalised width of 1.0. Also shown are field plots for the optimised width of 0.7 and experimental width of (c) 1.0.

5. Conclusion

In conclusion, we have shown the novel approach of using the mini-stopband (MSB) of a W3 photonic crystal waveguide as a stand-alone laser mirror in a GaAs based device. Selective feedback from the MSB results in single transverse mode output, even for wide gain sections and high operating currents. The thresholds are similar to lasers with two cleaved facets, but optimising the interface between the access waveguide and the W3 can lead to a fourfold increase in reflectivity and should reduce threshold currents significantly. This unique design opens a wide range of potential applications and provides an excellent platform for the integration of additional components, such as photonic crystal cavities to act as etalons, as well as the ability of operating high power, broad area lasers in a single mode. The W3 mirror could also be used as a dispersion element or group-delay element by chirping the crystal period or the hole radius.

Acknowledgments

The authors would like to thank G. Robb and S. Balfour for their help with experiments. T. P. White is supported by an 1851 Royal Commission Research Fellowship. L. O'Faolain is supported by the EU-FP6 NoE ePIXnet.